Adaptive localization for robot manipulators

Teng-Hu Cheng, Yin-Long Yan, Zhe-Hui Chen, Chien-Yu Wu, Shu Huang, and Chin-Chi Hsiao*

***Abstract*—Under the development of aviation heavy industry, the accurate position of robot depends on laser odometry. However, there are some limitations about using laser odometry in practice: 1. complicated pre-processing and calibration 2. Limited to plain and simple environment 3. Expensive manufacture and maintenance. Therefore, this study developed a visual and inertial system to achieve the objective without less cost. To this end, a light-weight and low-cost visual-inertial localization method is applied to achieve the requirement of the high accuracy of the industry robot.**

I. Introduction

Under the demands on energy saving and light-weighted products, aluminum and composite materials have been gradually adopted to replace heavy-weighted steel materials. This change of adoption of raw materials is especially significant for automotive and aerospace industries. In contrast to traditional application specific machinery equipment, industrial robots are more flexible and are more suitable in reconfigurable smart manufacturing system. With the continuous improvement of industrial robot technology, robotic machining will be applied to more machining applications[1].

Industrial robots on flexible and reconfigurable issues, they are appropriate to develop manufacturing systems which are helpful to perform automatically operation such as cutting, drilling, grinding, polishing, milling, and deburring. Industrial robots are applied in the field of aviation manufacturing with the continuous advancement of industrial robot technology. But some problems have also been exposed, such as insufficient accuracy of robots and too many processing points[2]. Therefore, industrial robots need to be more intelligent to meet the requirements in the manufacturing area.

The current industrial robots have good repeatability, ranging from ±0.02 to ±0.3 mm. However, in machining applications, it mainly depends on the accuracy of the trajectory accuracy (dynamic/continuous point position) of the industrial robot, instead of the repeatability of the robot. Unfortunately, robot manufacturers usually do not provide accuracy and trajectory accuracy specifications. The accuracy of the robot roughly falls between a few mm to 10 mm [3]. In most manufacturing applications, robot accuracy and trajectory accuracy are prerequisites and mandatory.

We develop a method that fuses visual odometry and a 6-DOF IMU by solving an optimal algorithm, and the estimated robot position is guaranteed by this algorithm. This method can be applied to the machining field or more other related field.

In this study, the accuracy of the robot is corrected by a light-weight and lower-cost positioning equipment. The fusion of the 3D camera and the IMU sensor can improve the average accuracy of robot positioning (≤ 1 mm). In some applications, it can replace the existing high-cost laser positioning correction method. In order to accurately improve the accuracy of the robot, the sampling frequency of the 3D camera must be greater than 100 Hz, and the calibration time must be less than 10 minutes.

The rest of the paper is organized as follows. We briefly describe the ways to improve the accuracy of the robot in Section II. The detailed method fusing the measurement data from IMU and camera to estimate an optimal position of feature point is described in Section III. Finally, the experiment results are listed in Section IV, followed by a conclusion in Section V7.

II. Technical Gaps/Compensation Methods for Industrial Robots Used in Machining

Basically, there are two methods to improve the accuracy of the robot. The first method is kinematic model correction, and the other is external sensor correction.

A. Kinematic Model Calibration

The economically feasible solution to improve the absolute accuracy of the robot is through the calibration procedure. The method is to identify and compensate the geometric and non-geometric errors in the robot structure. Because these internal errors are usually not easy to measure directly, they must be identified indirectly through attitude errors and the associated mathematical model (DH Model). After constructing the DH Model, the robot is ordered to multiple positions in the

Teng-Hu Cheng received the Ph.D. degree from the Department of Mechanical Engineering, University of Florida, Gainesville, FL, USA, in 2015.,In 2016, he joined the Department of Mechanical Engineering, National Chiao Tung University, Hsinchu, Taiwan (e-mail:tenghu@g2.nctu.edu.tw).

Yin-Long Yan received his B.S. from the Department of Mechatronics Engineering at the National Changhua University of Education, Taiwan, in 2019, and is currently a M.S. student in the Dept. of the Graduate Degree Program of Robotics at National Chiao Tung University, Taiwan. (e-mail: yanlong658.gdr08g@nctu.edu.tw).

Zhe-Hui Chen, was with National Chiao Tung University, Hsinchu, Taiwan. He is now with the Department of Mechanical Engineering, National Chiao Tung University. (email: v309611081.en09@nycu.edu.tw)

Chien-Yu Wu is with the Mechanical and Mechatronics Systems Research Laboratories, Industrial Technology Research Institute, Taiwan (e-mail:chienyuwu@itri.org.tw).

Shu Huang is with the Mechanical and Mechatronics Systems Research Laboratories, Industrial Technology Research Institute, Taiwan (e-mail: shu.huang@itri.org.tw).

Chin-Chi Hsiao* is with the Mechanical and Mechatronics Systems Research Laboratories, Industrial Technology Research Institute, Taiwan (886-3-5913896; fax:886-3-5913607; e-mail:hsiao_cc@itri.org.tw). *Corresponding author for this work

workspace, measures the real position and compares the posture error, and then calculates the internal error of the robot structure. After calibration, the error model can be used as a virtual sensor to measure and compensate for robot inaccuracies.

B. External Sensor Correction

Although it is possible to imitate the practice of the automobile industry, manually correct the accuracy with the aid of the teach pendant. However, it is not feasible in practice, because there are huge differences in the number of workpieces and operating procedures. In this case, it is too tedious or even impossible to use manual teaching methods to compensate for robot errors. Therefore, this research focuses on how to feed back the accuracy information of the external sensor(3D camera) to the robot system for further performance improvement.

III. LOW-COST VISUAL LOCALIZATION METHOD

First, define the state of the robot, as in equation (1)

$$\begin{aligned} X &= \left[X_0, X_1, \ldots X_n, X_c^b, \lambda_0, \lambda_1, \ldots \lambda_m\right] \\ x_k &= \left[p_{b_k}^w, v_{b_k}^w, q_{b_k}^w, b_a, b_g\right], k \in [0, n] \\ x_c^b &= \left[p_c^b, q_c^b\right] \end{aligned} \tag{1}$$

Where X_0, …, X_n are states to be estimated. X_k is defined as the state at time t_k. $p_{b_k}^w$, $V_{b_k}^W$ and $q_{b_k}^W$ are respectively the position, speed, and attitude of the arm end-effector at time t_k (world coordinate system). b_a and b_g are the deviation of accelerometer and gyroscope. p_c^b and q_c^b are the relative displacement and relative angle of the camera and the robot.

Second, the optimization problem is expressed as equation (2). The formula is the objective function for minimizing the error between measurement and model. The state function can be solved by nonlinear optimization methods (such as gradient descent method), where $p_{b_k}^W$ and $q_{b_k}^W$ are the optimized arm position and attitude.

$$\min_x \left\{ \begin{array}{l} \left\| r_p - H_p X \right\|^2 + \sum_{k \in B} \left\| r_B\left(\hat{z}_{b_{k+1}}^{b_k}, x\right) \right\|_{P_{b_{k+1}}^{b_k}}^2 + \\ \sum_{(i,j) \in B} p\left(\left\| r_C\left(\hat{z}_l^{cj}, x\right) \right\|_{P_{P_l}^{c_j}}^2 \right) \end{array} \right\} \tag{2}$$

The first term in equation (2) is initialization, and the second term is the error generated by the displacement integral of the IMU and the motion model, as in equation (3).

$$\begin{aligned} r_B(\hat{z}_{b_{k+1}}^{b_k}, x) &= \begin{bmatrix} \delta\alpha_{b_{k+1}}^{b_k} \\ \delta\beta_{b_{k+1}}^{b_k} \\ \delta\theta_{b_{k+1}}^{b_k} \\ \delta b_a \\ \delta b_g \end{bmatrix} \\ &= \begin{bmatrix} R_w^{b_k}\left(p_{b_{k+1}}^w - p_{b_k}^w + \frac{1}{2} g^w \Delta t_k^2 - v_{b_k}^w \Delta t_k\right) - \hat{\alpha}_{b_{k+1}}^{b_k} \\ R_w^{b_k}\left(v_{b_{k+1}}^w + g^w \Delta t_k - v_{b_k}^w\right) - \hat{\beta}_{b_{k+1}}^{b_k} \\ 2\left[(q_{b_k}^w)^{-1} \otimes q_{b_{k+1}}^w \otimes (\hat{\gamma}_{b_{k+1}}^{b_k})^{-1}\right]_{xyz} \\ b_{ab_{k+1}} - b_{ab_k} \\ b_{\omega b_{k+1}} - b_{\omega b_k} \end{bmatrix} \end{aligned} \tag{3}$$

The third term is the error produced by the camera measurement and the state estimation model to correct the actual displacement, as shown in equation (4). Although the integration of the second term will cause the error to accumulate, the error can be corrected back through the third formula.

$$\begin{aligned} r_c(\hat{z}_l^{cj}, x) &= \begin{bmatrix} b_1 & b_2 \end{bmatrix}^T \bullet \left(\hat{\bar{P}}_l^{c_j} - \frac{P_l^{c_j}}{\left\| P_l^{c_j} \right\|}\right) \\ \hat{\bar{P}}_l^{c_j} &= \pi_c^{-1}\left(\begin{bmatrix} \hat{u}_l^{c_j} \\ \hat{v}_l^{c_j} \end{bmatrix}\right) \\ P_l^{c_j} &= R_b^c\left(R_w^{b_j}\left(R_{b_i}^w\left(R_c^b \frac{1}{\lambda_l} \pi_c^{-1}\left(\begin{bmatrix} u_l^{c_i} \\ v_l^{c_i} \end{bmatrix}\right) + p_c^b\right)\right.\right. \\ &\left.\left. + p_{b_i}^w - p_{b_j}^w\right) - p_c^b\right) \end{aligned} \tag{4}$$

Finally, $p_{b_k}^W$ can be used to compute the error with the ground truth to evaluate the accuracy.

IV. EXPERIMENTAL RESULT

A. Camera coordinate system and image coordinate system

In order to understand the relationship between 2D image and 3D relative distance, it is necessary to understand the relationship between the camera coordinate system and the image coordinate system. Figure 1 is a schematic diagram of camera coordinates and image coordinates. P(X,Y,Z) is a point in the three-dimensional space observed in the camera coordinate system. The corresponding point where P is projected onto the image plane is $P_j(u, v)$.

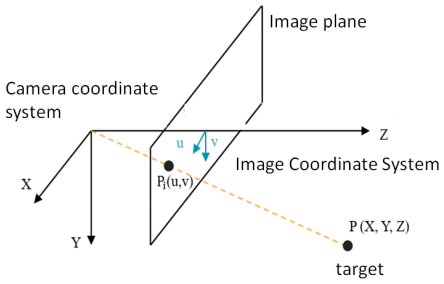

Figure 1. schematic diagram of camera coordinates and image coordinates

In general, the origin of the image coordinate is the upper left corner of the image plane, so there is a translational relationship between the camera coordinate system and the image coordinate system as shown in Figure 2.

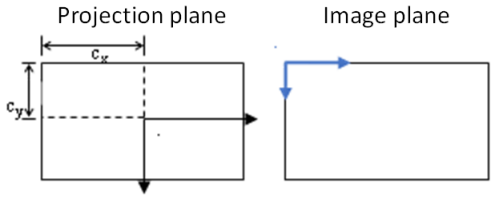

Figure 2. Schematic diagram of projection plane and image plane coordinates

Let f_x and f_y be the focal lengths in the X-axis and Y-axis directions respectively, and a homogeneous matrix can be produced.

$$\begin{bmatrix} u \\ v \\ w \end{bmatrix} = \begin{bmatrix} f_x & 0 & c_x \\ 0 & f_y & c_y \\ 0 & 0 & 1 \end{bmatrix} \begin{bmatrix} X \\ y \\ Z \end{bmatrix}$$

where $(u, v, w) = \left(\frac{f_x}{Z} + c_x, \frac{f_y}{Z} + c_y, 1 \right)$

B. Camera calibration

In order to correctly estimate the actual distance of the target object, the internal parameters of the camera f_x, f_y, c_x, and c_y need to be obtained first. Camera calibration can calculate the camera's internal parameter matrix (Intrinsic Matrix) and external parameter matrix (Extrinsic Matrix). The internal parameters can be obtained f_x, f_y, c_x, and c_y. The external parameters can obtain the rotation matrix of the camera relative to the world coordinate (including translation and rotation). Pinhole Camera Model can be expressed as follows:

$$s\begin{bmatrix} u \\ v \\ 1 \end{bmatrix} = \begin{bmatrix} f_x & 0 & c_x \\ 0 & f_y & c_y \\ 0 & 0 & 1 \end{bmatrix} \begin{bmatrix} r_{11} & r_{12} & r_{13} & t_1 \\ r_{21} & r_{22} & r_{23} & t_2 \\ r_{31} & r_{32} & r_{33} & t_3 \end{bmatrix} \begin{bmatrix} x \\ y \\ x \\ 1 \end{bmatrix}$$

When the focal length of the camera is fixed, the internal parameter matrix will not change with the movement of the object or the movement of the camera. From these data, the required image characteristics can be further obtained. Camera calibration package provided by ROS is used to calibrate the camera. Detailed calibration information is based on [4][5].

C. Image positioning

According to [6], the positioning system can be completed through a 3D camera and an inertial measurement system (IMU). In this system, the IMU and camera are fixed on the robot, as shown in Figure 3. As the robot moves, the actual position, distance and posture of the movement can be detected to provide information for assisting positioning. In this system, the distance of movement can be estimated through the feature points in the environment. In practice, artificial feature points (such as Apriltag) can be used to increase reliability. The fusion of the two sensors makes a higher positioning accuracy through the measurement of the camera's Odometry and IMU.

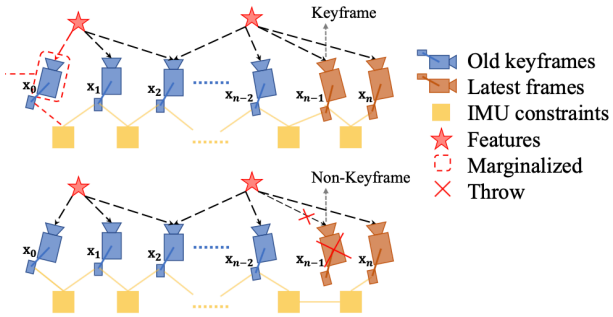

Figure 3. Visual inertia Odometry

D. Experimental result

In the experiment, a reflective ball and Laser Photosphere position will be installed on the robot, as shown in Figure 4. The high-speed camera positioning system is used to locate the end-effector of the robot, and the laser tracker is used for measurement at the same time. The measured value of the Laser tracker can be used as ground truth to obtain the error. Figure 5 shows the setup of the 3D camera.

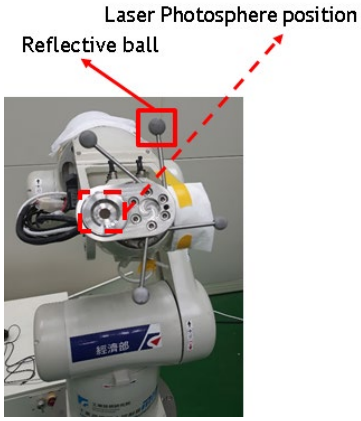

Figure 4. experiment setup : robot and reflective ball

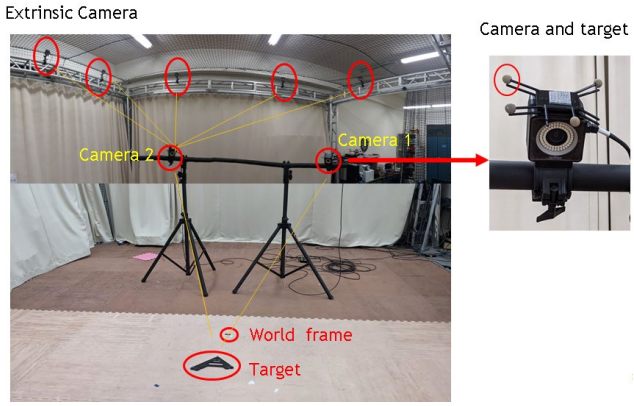

Figure 5. experiment setup : Camera

Since the coordinate systems of the two sensors are different, and the laser tracker lacks a posture measurement function. Therefore, the experimental design is to give 10 way points on a straight line trajectory, and stay on them for a while, and finally compare the position errors of the 10 way points, as shown in Figure 6. The reason of using this method is that a transformation between the frames of the two sensors through the 10 waypoints can be constructed. I shows the results of 9 experiments, the average error is about 0.53mm.

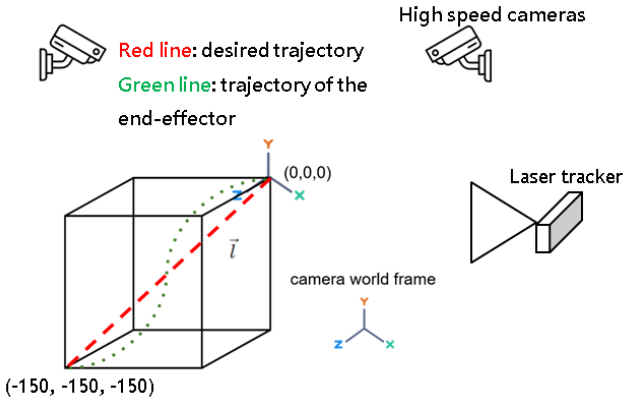

Figure 6. Experiment description

Table I. Experimental Statistics

No. of experiment	Real distance (mm)	Measured distance (mm)	Absolute error (mm)	Error (%)
1	20	18.33	1.67	8.35
2	20	19.96	0.04	0.2
3	20	18.40	1.6	8
4	20	20.10	0.10	0.5
5	20	20.26	0.26	1.3
6	20	19.41	0.59	2.95
7	20	19.88	0.12	0.6
8	20	19.15	0.85	4.25
9	20	19.74	0.26	1.3
Ave.	20	19.47	0.53	2.65

V. Conclusion

In this study, estimation algorithms and optimization algorithms are used to enable the robot to ensure high-precision positioning through the calibration of measuring instruments (general accuracy). Compared with the existing laser positioning method, the visual sensor fusion method can reduce the cost. The pre-positioning work can be simplified, and there is no need to spend time installing too many large instruments. According to the experimental results, the average error after correction is 0.53 mm. Through the trajectory of the robot and the real-time positioning of this method, it can be inferred which angle of the robot will cause a large positioning error. In the future, the cause of the problem can be analyzed (e.g., motor, reduction mechanism, and controller). In this study, 3D vision is used to assist the positioning of the robot. In addition to improving the positioning accuracy of the robot. In the future, sensors can be combined with automatic calibration to reduce manpower requirements and gradually develop towards Industry 4.0.

Acknowledgment

Thanks to the support of the Department of Industrial Technology (Project Number:K353C80000), so that this research can be carried out smoothly.

References

[1] I. Iglesias, M.A. Sebastián, J.E. Ares, “Overview of the state of robotic machining: Current situation and future potential”, The Manufacturing Engineering Society International Conference, Procedia Engineering, Procedia Eng 132, p911-917, 2015.

[2] Brian Rooks,"Automatic wing box assembly developments", I n d u s t r i a l R o b o t : A n International Journal, vol. 28 no, 4, pp.297- 302, 2001.

[3] Siciliano, B., Khatib, O., Handbook of Robotics, Springer, 2008.

[4] Camera Calibration, http://wiki.ros.org/camera_calibration

[5] Camera Calibration With OpenCV, https://docs.opencv.org/2.4/doc/tutorials/calib3d/camera_calibration/camera_calibration.html

[6] T. Qin, P. Li, and S. Shen, “VINS-Mono: A Robust and Versatile Monocular Visual-Inertial State Estimator,” *IEEE Transactions on Robotics*, vol. 34, no. 4, pp. 1004-1020, 2018.